Carrier Free Delivery System of Monoacylglycerol Lipase Hydrophobic Inhibitor for Cancer Therapy

Adeel Muhammad
Ca'Foscari University of Venice: Universita Ca' Foscari
Gloria Saorin
Ca'Foscari University of Venice: Universita Ca' Foscari
Giacomo Boccalon
Ca' Foscari University of Venice: Universita Ca' Foscari
Andrea Augusto Sfriso
University of Ferrara: Universita degli Studi di Ferrara
Salvatore Parisi
University of Trieste: Universita degli Studi di Trieste
Isabella Moro
University of Padua: Universita degli Studi di Padova
Stefano Palazzolo
National Cancer Institute CRO Aviano: Centro di Riferimento Oncologico
Isabella Caligiuri
National Cancer Institute CRO Aviano: Centro di Riferimento Oncologico
Carlotta Granchi
University of Pisa: Universita degli Studi di Pisa
Vincenzo Canzonieri
National Cancer Institute CRO Aviano: Centro di Riferimento Oncologico
Tiziano Tuccinardi
University of Pisa: Universita degli Studi di Pisa
Flavio Rizzolio (flavio.rizzolio@unive.it)
Ca' Foscari University of Venice: Universita Ca' Foscari https://orcid.org/0000-0002-3400-4363

Research

Keywords: Monoacylglycerol lipase (MAGL), Cancer, Therapeutic Target, Delivery System, Hydrophobic inhibitor, nano crystals

Posted Date: April 6th, 2021

DOI: https://doi.org/10.21203/rs.3.rs-373238/v1

Abstract

Background: Monoacylglycerol lipase (MAGL) is an emerging therapeutic target for cancer. It is involved in lipid metabolism and its inhibition impairs many hallmarks of cancer including cell proliferation, migration/invasion and tumor growth. For these reasons, our group has recently developed a potent reversible MAGL inhibitor (MAGL23), which showed promising anticancer activities. Here in, to improve its pharmacological properties, a nanoformulation based on nanocrystals coated with albumin was prepared for therapeutic applications. MAGL23 was solubilized by a nanocrystallization method with Pluronic F-127 and Cetyltrimethylammonium bromide (CTAB) as surfactants into an organic solvent and was recovered as nanocrystals in water after solvent evaporation. Finally, the solubilized nanocrystals were stabilized by human serum albumin to create a smart delivery carrier.

Results: An in-silico prediction (lipophilicity, structure at different pH and solubility in water), as well as experimental study (solubility), have been performed to check the chemical properties of the inhibitor and nanocrystals. The solubility in water increases from less than 0.01 mg/mL (0.0008 mg/mL, predicted) up to 0.82 mg/mL in water. The formulated inhibitor maintained its potency in ovarian and colon cancer cell lines as the free drug. Furthermore, the system was thoroughly observed at each step of the solubilization process till the final formulation stage by different spectroscopic techniques and a comparative study was performed to check the effects of Pluronic F-127 and CTAB as surfactants. The formulated system is favorable to release the drug at physiological pH conditions (at pH 7.4, after 24h, less than 20% of compound is released).

Conclusions: As per our knowledge, we are reporting the first ever nanoformulation of a MAGL inhibitor, which is promising as a therapeutic system where the MAGL enzyme is involved, especially for cancer therapeutic applications.

Background

Drug design and combinatorial chemistry have been exploited to develop new drugs, which are generally characterized by high molecular weight, lipophilicity that assist drug to transfer across membranes [1] and therefore low solubility in water [2]. Indeed 40-70% of new molecules developed in the context of drug discovery programs are not enough soluble in aqueous media, thus compromising the bioavailability of the drug [3]. Therefore, in order to became commercially available (in general almost 10-17 years after its first synthesis [4]) a poorly soluble drug needs to be formulated through drug delivery technologies.

Many drug discovery programs are dedicated to cancer treatment, which is the second major disease that kills thousands of people around the globe every year. Indeed, despite several therapeutic strategies have been employed to cure cancer, there is still no accurate way to eradicate it by roots [5,6] and chemotherapy which is considered one of the major treatment tools, suffers from several issues and even failure [7,8]. To overcome traditional chemotherapy issues, current approaches are focused on the discovery of drugs that target specific receptors or proteins mostly upregulated in tumor cells. This

strategy takes part of a wider concept termed personalized therapy in which each patient is treated with specific targeted drugs based on the genotype and phenotype. Several research groups are exploring many genes, receptors, and enzymes that are commonly involved in many cancer types and could be a therapeutic target [6,9,10]. Among the enzymes, monoacylglycerol lipase (MAGL) is a member of the serine hydrolase superfamily, which primarily degrades the endocannabinoid 2-arachidonoylglycerol (2-AG) to arachidonic acid and glycerol in the brain, thus interrupting its signaling on cannabinoid receptors. MAGL is also involved in the hydrolysis of monoacylglycerols in peripheral tissues [11]. For this reason, in cancer cells MAGL was reported to activate oncogenic signaling related to the intracellular pool of free fatty acids [12] and it proved to be involved in sustaining the growth of different cancer cells [13–15]. Recently, our group developed a reversible and selective MAGL inhibitor (MAGL23, Figure 1), which inhibits the target enzyme with a potency in the nanomolar range (K_i = 39 nM) [16]. MAGL23 is a compound with suitable properties to be further developed as a drug because it is obtained by a few steps' synthetic preparation. Moreover, its reversible binding mechanism makes it devoid of the typical side effects of irreversible MAGL inhibitors observed in *in vivo* studies [17]. Finally, it also showed selectivity for MAGL inhibition over the other main components of the endocannabinoid system, i.e., cannabinoid receptor 1 and 2, fatty acid amide hydrolase, α/β hydrolase-6 and α/β hydrolase-12. Interestingly, the ability of MAGL23 to inhibit the viability of ovarian, colon, and breast cancer cell lines was demonstrated [16].

Although the results in terms of antiproliferative activity in cancer cells were quite good (IC_{50} values in the low micromolar range), the inhibitor suffered of problems related to poor solubility. Recently, nanotechnology is playing a vital role to improve important drug parameters such as solubility, biodistribution, pharmacokinetics and pharmacodynamics [18–22]. Among the possible approaches to increase the solubility, nanocrystallization allows to avoid a matrix such as polymeric or lipid nanoparticles. Indeed, drug nanocrystal particles have an almost 100% hydrophilic surface, avoiding the toxic effects of the matrix and with a high yield of solubilization [23,24]. In nanotechnology, two different approaches can be exploited: the "Top-down" and "Bottom-up" methods. When applied to crystals, the main concept is to reduce their size from several microns to a few nanometers that are easily soluble in water. The "top-down" approach foresees the use of high shear stress for the breakage of large crystals while in the "bottom-up" approach, the nanocrystals are generated from the crystallization of drug molecules. Furthermore, the two processes can be used one after the other in a combination process, where usually after a "bottom-up" process of crystallization, size is decreased with a "top-down" method such as ultrasonication [25]. However, these methods still have limits due to the variation in the size of nanocrystals during batch preparation and the chemical nature of the compounds [26–28].

Recently, Park et al. introduced a novel nanocrystallization strategy for the solubilization of poorly soluble drugs in water by a combined method. The authors used the Pluronic F-127 and cetyltrimethylammonium bromide (CTAB) as surfactants to obtain a controlled generation of the nanocrystals in water and then covered them with human serum albumin [27]. The presence of surfactant during the crystallization allows to control the size of the obtained nanocrystals. More importantly, the bare nanocrystals of

therapeutic compounds can lead to the adsorption of non-specific proteins resulting in the uptake by mononuclear phagocyte system (MPS) [29]. Despite the fact that others hydrophilic stealth surfaces could reduce the MPS uptake of nanocrystals, there would always be a possibility that after the distribution of nanocrystals in tumors, they could interfere with the retention and intended cellular interactions [30]. On the contrary, albumin is a natural carrier of native ligands and other hydrophobic molecules, it is very stable, digestible and decomposable by cells, provides amino acids for cell metabolism and helps to internalize the nanocrystals in tumoral sites through the interaction with specific receptors [31–34].

In the proposed study, it was utilized a combined method to obtain nanocrystals of the MAGL23 inhibitor that was highly hydrophobic. The inhibitor was solubilized with Pluronic F-127 or CTAB surfactants in the organic solvent (chloroform) and the crystals were obtained by sonication in water. We compared the effects of surfactants and the interaction of albumin with the MAGL23 inhibitor. The system was observed at each step of the formulation by using different spectroscopic techniques to ascertain the stability of the formulation. We believe that the proposed system provides an opportunity to increase the solubilization of poorly soluble hydrophobic drugs, such as MAGL23 inhibitor, and create a drug delivery system for in vivo applications.

Results And Discussion

Nano crystallization process increases the solubility of MAGL23

MAGL23 is an organic molecule of medium molecular weight (369.436 g/mol) which, basing on the Chemicalize.com prediction (predicted physicochemical properties are reported in Table 1), is highly hydrophobic and insoluble at physiological pH levels (Figure 2a) at which it is mainly in its neutral form (94% at pH=7.4) (Figure 2b). In order to confirm the poor solubility of MAGL23 at neutral pH, a solubility test was performed on drug powder, following the method reported in section 2.2. The experimentally determined solubility is lower than 0.01 mg/ml (the lowest measurable value) in accordance with the prediction.

logP	4.18
Isoelectric point	3.50
Intrinsic solubility	0.808 µg/ml
pKa (strongest acid)	8.63
pKa (strongest base)	-1.64

Table 1. Physicochemical properties of the drug predicted (by Chemicalize.com)

Despite the fact that neutral compounds (having zero charges) are more favorable for biological membrane penetration than energetically charged compounds [4,35], poor solubility is often an

impediment for the development and the clinical use of a drug. The drug formulation for enhancing aqueous dispersion often require the use of surfactants or nanoparticles, which may result in an increased systemic toxicity of the drug [36]. Nanocrystals having an high ratio between the carried drug and the excipients avoid toxicity and deliver a substantial amount of drug to the cells [24]. In fact, to overcome MAGL23 solubility issue, the drug was formulated as nanocrystals covered by albumin, which strongly binds to lipophilic drugs [24]. Wrapping MAGL23 nanocrystals with albumin was important for the safe delivery without a toxic nanocarrier and helped to stabilize and to internalize the nanocrystals into the cells [27]. The formulation proposed with both surfactants led to a significant increase in drug solubility as experimentally confirmed, reaching 0.82±0.06 mg/mL with at least eighty-fold increase of solubility in comparison with the stand-alone drug.

Yield and coating

The absorbance in the UV region was utilized to measure the loading of the MAGL23. Six separate synthesis were performed; Table 2 shows the average of the percentage of yield for each analyzed compound and the average of the percentage of HSA bonded to MAGL-AF and MAGL-AC nanocrystal samples. The results showed that the nanocrystallization protocol solubilizes MAGL23 up to 0.82 mg/ml and the percentage of HSA bound to the nanocrystals were 22% and 34% by weight in MAGL23-AF and MAGL23-AC, respectively.

Samples	Yield (%)	% bonded HSA
MAGL23-F	82 ± 6	-
MAGL23-AF	59 ± 7	22 ± 4
MAGL23-C	76 ± 4	-
MAGL23-AC	58 ± 6	34 ± 11

Table 2. Percentage yield of nanocrystal samples and percentage of interacting HSA (data are reported as mean ± standard deviation).

Morphological Analysis

The morphological analysis was performed by transmission electron microscopy (TEM) on nanocrystal samples and drug powder (MAGL23). The formulation with both surfactants produced a reduction in crystal size with similar size frequency distributions (Figure 3 a,b,c) with average sizes of 389 nm (95% CI: 336-442) and 391 nm (95% CI: 344-439) for MAGL23-AC and MAGL23-AF, respectively. The images of nanocrystal samples at intermediate state of formulation (MAGL23 and MAGL23-F) are reported in supporting information Figure S1. Clearly, the size decreased and monodispersibility increased compared to MAGL23 while employing pluronic acid as surfactant.

Dispersion and homogeneity of the crystals were evaluated for MAGL23-AF and MAGL23-AC (Figure 3 d,e,f). TEM data support the fact that surfactants allowed to increase the solubility of the drug by creating smaller and more monodisperse nanocrystals with a hydrophilic coat. The size of MAGL23-AF suspended particles measured using DLS technique was around 395.4 nm (PdI 0.1), a value close to that identified by analysis on the TEM pictures, highlighting good dispersion of the crystals. Conversely, the hydrodynamic diameter of MAGL23-AC measured by DLS was bigger with an average crystal size of 477.2 nm (PdI 0.2) and it could be due to self-agglomeration of the particles in solution as it was possible to ascertain from in vitro observations. This unfavorable behavior and the higher toxicity of CTAB (see IC_{50} results, Table 3) led us to proceed further with pluronic F127 formulation only.

Characterization of nanocrystals, MAGL23 and coating components

The nano-crystallization process should not change the chemical and structural properties of the drug to maintain its efficacy, while increasing its pharmacokinetic properties by size reduction and coating.

To investigate the structure of the nanocrystals and study them during the crystallization process, X-ray diffraction (XRD) measurements were performed. XRD diffractograms of nanocrystal samples MAGL-F, MAGL-AF and MAGL23 are reported in Figure 4a for values of 2θ ranging from 10 to 40° since for higher value of 2θ there were no peaks. Nanocrystals samples and MAGL23 diffractograms show intense and sharp diffraction peaks, which evidence their crystalline structure. All the major peaks of MAGL inhibitor diffractogram are present in nanocrystal samples, at 2θ values of 13.5, 15.75, 17.95, 18.95, 19.75, 23.5°, despite the dilution effect influences the nanocrystals samples. These results indicate that the crystallization process did not interfere with the inner crystalline structure of the drug.

To assess the possible interactions between the drug and the surfactants present on crystal surface in the nanocrystal formulation, FTIR spectroscopy analysis were performed for nanocrystal samples and MAGL23 (Figure 4b). Nanocrystal samples (MAGL-AF and MAGL-F) show mostly all MAGL23 bands (around 3430 cm^{-1} OH, 3167 cm^{-1} aromatic CH, 2865,2929,2961 cm^{-1} aliphatic CH, 1683 cm^{-1} chetonic CO, 1621 cm^{-1} ammidic CO, 1320 cm^{-1} CF [37]) without any significative shift. The only difference is the strong band at 3438 cm^{-1} steeper in MAGL-F and MAGL-AF, evidencing the presence of water in the samples probably due to the incomplete lyophilization [38,39]. The Pluronic F-127 weak band at 1100 cm^{-1} in MAGL-F is the only coating components band visible in the nanocrystal samples. Therefore, FTIR spectra evidence that the chemical structure of the drug remains unchanged during the crystallization process and that the drug delivery system is mainly formed by the active compound with little amount of coating components not strongly interacting with it. The chemical stability of MAGL23-AC and MAGL-C were also tested by FTIR spectra (supporting information Figure S2). No change was observed in the structure even by employing CTAB as surfactant.

Eventually, the FTIR and XRD spectra evidenced that during the crystallization process, the drug remained chemically and structurally unchanged and the drug delivery system was mainly formed by the active compound.

MAGL23-AF has an optimal release profile

MAGL23-AF in vitro release test results are reported in Figure 5 as percentage of the released drug over the initial drug amount. It is evident that the dissolution rate is low. Indeed, after one day only the 19 ± 7% of the drug was released and this value reached the 42 ± 6% after three days. The low release rate is in agreement with the stability of the complex [40]. This means that the nanocrystal formulation allows to increase the solubility, avoiding burst release of the drug and toxic effects during the blood circulation site. Taking advantages from the Enhanced Permeability Retention (EPR) effect and the targeting ability of the albumin, the drug should be released mainly at the targeted site reducing the side effects and promoting the uptake in cancer cells over more cycles of cell division [41,42].

Cell viability assay

MAGL enzyme is overexpressed in a large variety of cells deriving from ovarian and colorectal cancers, and also has a key role in tumor progression [43,44]. Therefore, the new formulations of MAGL23 were tested on tumor cell lines inherent to ovarian [45] (A2780, Skov3 and Ovcar3) and colorectal [46] cancers (Colo205 and HCT116).

Before testing MAGL23 nanocrystals, pluronic acid F127 and CTAB were evaluated. The IC_{50} values are reported in the Table 3. The IC_{50} of the CTAB are significantly lower than those of F-127, which suggests a marked self-cytotoxic activity. Conversely, pluronic acid F-127 did not display a significant cytotoxic activity and should be considered the best biocompatible formulant [47,48] among those tested. We therefore focused only on compounds treated with F-127, as a biocompatible surfactant with low intrinsic cytotoxicity. In Table 3 are reported the calculated IC_{50} values of MAGL23 initially dissolved in DMSO and MAGL23-AF dissolved in aqueous solution. In general, IC_{50} values were in the same range for each tumor cell line treated with MAGL23-AF compared to MAGL23 stand-alone.

Cell Line	IC_{50} (μM)			
	MAGL23	MAGL23-AF	CTAB	F-127
A2780	4.0±2.0	4.1 ± 0.4	0.6 ± 0.3	>200
SKOV3	15±2*	37 ± 9	0.35 ± 0.03	>100
OVCAR3	57 ±2*	23 ± 13	0.04± 0.01	>200
COLO205	3.0 ± 0.5	27 ± 6	0.042 ± 0.002	>200
HCT116	21 ± 1.0*	16± 2	1.1 ± 0.4	>200

Table 3. Calculated IC_{50} results for drug solution, nanocrystals samples and surfactants (data are reported as mean ± standard deviation).* Data from reference [16]

MAG23-AF and MAGL23 have comparable efficacy, in agreement with the results obtained from the nanocrystal characterization, which evidenced the maintenance of structural and chemical characteristics of the drug during the nanocrystallization procedure. Therefore, the drug delivery system allows to increase the water solubility without perturbing the molecule and consequently maintaining unaltered its activity on cells. Furthermore, the albumin coating should improve the biodistribution *in vivo* because albumin works first of all as a carrier to transport molecules in the blood [49,50], and secondly because albumin has a high affinity with sialoglycoprotein gp60, a protein present in the vascular endothelium and closely related to the formation of caveoles and transcytotic processes and SPARC (Secreted Protein, Acidic and Rich in Cysteine), which are overexpressed in the tumors [42,51,52]. These characteristics allow MAGL23-AF to extravasate more easily in vivo than MAGL23, significantly increasing the possibility of concentrating the drug around the tumor mass and therefore improving its effectiveness.

MAGL23-AF internalized into the cells through lysosomes

To determine the intracellular localization of MAGL23-AF, A2780 cells were probed with Hoechst 33342 (blue nucleus) and Lysotracker (green Lysosomes). MAGL23-AF was probed with rhodamine as reported previously [27]. A time course analysis at 1 hour and 24 hours showed that MAGL23-AF accumulates in the lysosomes with a Pearson's correlation coefficient (R) of 0.73 and 0.67, respectively (yellow signals, Figure 6). These data suggest an active mechanism of cellular import with a partial trafficking to lysosomes (Figure 6).

Conclusions

The first nanoformulation of a potent MAGL inhibitor, MAGL23, which is a promising compound as anticancer agent, was developed. MAGL is an enzyme that is highly expressed in tumors, where it plays a fundamental role in the oncogenic lipid signaling that promotes invasion, migration, survival, and in vivo tumor growth [12]. Many MAGL inhibitors have been reported in the literature and they showed positive effects when tested in in vivo studies. However, most MAGL inhibitors act by an irreversible mechanism of action, which provokes many negative effects in animal models, thus hampering their further development as drugs [17]. On the other hand, potent MAGL reversible inhibitors are usually characterized by a high lipophilicity. MAGL23 is a recently published reversible MAGL inhibitor, whose development is facilitate by its high selectivity towards other members of the endocannabinoid system as well as by its straightforward synthetic preparation [16]. Unfortunately, not a single delivery system is available (for reversible and irreversible inhibitors). A challenge in drug delivery systems is to have one single system able to protect and transport the drug to the target site without compromising the potency. Most of the systems are not stable in *in vivo,* suffer of a low loading efficiency and require drug pre-solubilization (because of their intrinsically hydrophobic nature). Hence, a nanocrystallization method was employed to

decrease the size of the crystals of MAGL23. They were dissolved in an organic solvent together with different surfactants, which helps to decrease the size of nanocrystals and provides their hydrophilicity, in turn increasing the solubility at about 1 mg/ml. Usually, the pharmacokinetics profile of the therapeutic compounds is altered by decreasing the size (while employing different physical or chemical methods to achieve the solubility) in turn influencing the potency of the compound. But in our case, the nanocrystal formation was thoroughly observed by different spectroscopic techniques and results demonstrated that there was no change in the structural properties and the IC_{50} data on cells are also in line with the results obtained with the compound stand-alone. The nanocrystals were formulated with albumin for safe delivery applications. Indeed, albumin can direct the therapeutic compound at tumoral sites via the GP60 receptor and SPARC, and also it stabilizes the nanocrystals avoiding unwanted protein adsorption during circulation in the body. Furthermore, our future research is directed to investigate the *in vivo* properties of the formulated nanocrystals in animal models. In conclusion, in this article, we developed the first soluble and easily absorbable nanoformulation system for a potent reversible MAGL inhibitor for a future use in clinical applications.

Materials And Methods

Lyophilized powder of albumin from human serum albumin (HSA) ≥96% (Cat n° A3782), hexadecyltrimethylammonium bromide (CTAB) ≥ 98% (Cat n° H5882), powder of Pluronic® F-127 (Cat n° P2443) suitable for cell culture and acetonitrile (Cat n° 151807) were purchased from Merck, Darmstadt, Germany. To perform Bradford protein assay, dye reagent (Cat n° 500-0006) was purchased from Bio-Rad, Hercules, CA, US; methanol (Cat n° A177150010) for LC/MS was purchased from Carlo Erba, Milan, Italy; chloroform (Cat n°67-66-3) from Thermo Fisher Scientific, Waltham, MA, US. Water was purified with Milli-Q® (Millipak® 0.22µm) system. Compound MAGL23 was synthetized as previously reported [16].

Nanocrystallization and Albumin Formulation

The nanocrystallization of MAGL23 was performed by the method reported in the literature [27]. Briefly, 6 mg of the drug and 24 mg of Pluronic F-127 (F-127) were mixed in 3 mL of chloroform inside a round-bottom flask. The mixture was carefully mixed to ensure the drug dissolution, then chloroform was evaporated in a rotary evaporator at 30°C until a thin amorphous layer of the mixture was obtained. The sample was recovered in 6 mL of milli-Q water achieving a final drug concentration of 0.82 mg/ml. Bath sonication (1 min) and probe sonication (10 min, 40% frequency, in a mixture of ice and water to avoid heating the sample) were used to form nanocrystals from the thin film and to homogenize the sample. This method was replicated also replacing 24mg of F-127 (MAGL23-F) with 2.4 mg of CTAB (MAGL23-C).

In the second step, 4 mg of HSA were added for each mL of the solution containing water-soluble nanocrystals of drug. Each mL of the mixture was left in rotation at 30 rpm, room temperature, for 24h to ensure the maximum coverage and interaction between HSA and nanocrystal surface. The nanocrystal samples were washed two times by centrifugation at 38000 rpm, 4°C for 1h to remove the unbounded

albumin and extra surfactants. The pellet obtained after the second centrifuge was lyophilized and resuspended in milli-Q water while maintaining the same starting volume. MAGL23-C plus HSA were later referred as MAGL23-AC while the ones obtained from MAGL23-F as MAGL23-AF.

Solubility Test

The solubility of the MAGL23 inhibitor was tested in silico as well as experimentally. The in silico prediction was performed by the “Chemicalize” software (Chemicalize.com; ChemAxon Ltd., Budapest, Hungary) while experimental results were obtained by mixing 1 mg/mL of drug powder in milli-Q water for 1 hour. The solution was centrifuged at 10000 rpm for 10 minutes to eliminate the insolubilized fraction and quantified through UV-Visible spectroscopy method.

Yield and coating

The nanocrystals were analyzed spectrophotometrically in the UV region at 252 nm using the Agilent 8453 spectrophotometer through a calibration curve method. Samples solutions of MAGL-C and MAGL-F were diluted in methanol to be quantified. The concentrations of MAGL23-AC and MAGL23-AF were measured by diluting the solution in methanol, following by centrifugation (12000 rpm, 2 min) to precipitate HSA and then quantifying the drug in the supernatant. The yield % of the nanocrystal formulation was determined as the concentration of the nano crystallized material, over the quantity of the drug used for the nanocrystal production, the ratio was multiplied by 100. The quantity of HSA in MAGL23-AF and MAGL23-AC was determined by Bradford protein assay (Bio-Rad reagent) using the Agilent 8453 spectrophotometer (λ=595nm) by comparison with a HSA calibration curve. The percentage of HSA bound to MAGL23-AF and MAGL23-AC, was calculated by dividing the albumin concentration in the sample, by the concentration of the drug encapsulated in the nanocrystals and multiplying by 100.

Morphology, Size, and Structural Analysis

XRD analysis

After spectrophotometric quantification, compounds were re-centrifuged at 38000 rpm for 1h, then the supernatant was discarded, and the pellet was lyophilized. The obtained powders, and the original drugs were analysed by Philips X-ray diffractometer with PW1050/70 goniometer. CuKα radiation (λ = 1.54178Å) was used, the diffractograms were recorded by setting a diffracted intensity detection step equal to 0.05°. The unit of measurement of the detected intensity is the number of pulses / second. In order to compare the spectra they have been normalized, the signal to noise ratio is influenced by the quantity of the samples used for the measurement.

FTIR analysis

Solid nanocrystal samples were obtained as already described in X-ray diffraction technique section. The lyophilized samples of nanocrystals were used to prepare the pellet with KBr. Fourier-transform infrared (FTIR) spectrum were measured with FTIR spectrophotometer (Perkin Elmer-Spectrum One).

TEM analysis

A drop of solution (about 25 µl) was deposited on a 400-mesh holey film grid; after staining with 1% uranyl acetate (2 min), the sample was observed with a FEI Tecnai G2 transmission electron microscope operating at 100 kV (Hillsboro, Oregon, US). The images were taken with a Veleta digital camera (Olympus Soft Imaging System). Image processing to outline crystals and coating proteins and to measure Feret diameter was carried out by ImageJ (1.52a) software (the point-by-point set of operations for image processing is described in a dedicated section of the supplementary material).

Dynamic light scattering analysis

Dynamic light scattering (DLS) analysis were performed by Zetasizer Nano particle analyzer (Malvern Panalytical, Malvern, UK) on nanocrystals samples diluted with Phosphate-buffered saline (PBS).

In vitro testing

Cell viability

Ovarian cancer (A2780, KURAMOCHI, SKOV3, OVCAR3) and colorectal cancer (Colo201, Colo205, HCT116) cell lines and lung fibroblasts (MRC-5) were grown at 37 °C in a controlled atmosphere containing 5% CO_2 according to the supplier instructions. A thousand of cancer cells were plated in 96-multiwell culture plates or 5000 cells for MRC-5. The day after seeding, drugs were added with a serial dilution 1:10 to have a final concentration ranging from (100 µg/mL) to (0.001µg/mL). Cell viability was measured with Tecan Infinite M1000 PRO (Tecan, Mannedorf, Switzerland) after 96h with CellTiter-Glo® assay according to the supplier (Promega, Madison, WI, US). IC_{50} values were calculated from nonlinear regression dose-response curves by GraphPad Prism 8 Software. Averages were obtained from triplicates and the errors are standard deviations.

Drug Release

In order to reproduce in vivo conditions, the release test was performed dialyzing 1 mL of MAGL23-AF against PBS (pH 7.4, isotonic solution) placing the nanocrystal sample in a Slide-A-Lyzer MINI Dialysis Device 20k MWCO (Thermo Scientific) kept at 37°C. Aliquots of the solution were sampled at different time points and then measured with Agilent 1260 Infinity II HPLC with Variable Wavelength Detector, equipped with an Accucore-150-C18 column (5 cm x 2.1 mm, particle size 2.6 µm) (Thermo Fisher Scientific, Waltham, MA, US). A mixture of acetonitrile and MQ water 50:50 was used as mobile phase

with a flow rate of 0.5 mL/min. The quantification of the inhibitor has been obtained measuring the absorbance at 252 nm through a calibration plot. Aliquots were processed before HPLC analysis to remove HSA. The nanocrystal samples were diluted into acetonitrile and centrifuged at 13000 g for 15 minutes, then the supernatant has been diluted 1:1 with MQ water.

Lyso tracker analysis

The internalization and localization of the drug nanocrystals into the cells were analyzed. Typically, 150,000 cells were plated on top of a sterile coverslip into transparent microplates wells. The fluorescent dye rhodamine B was mixed at 30 µg/mL with nanocrystals under continuous rotation at room temperature for one hour. Then, 50 µg/mL of the rhodamine B-nanocrystals were added into each well for different time points (1h, 6h, and 24h). After incubation, the media was removed from the cells and new media was added with 200 nM of Lysotracker^{TM}Green DND-26 (Thermo Fisher Scientific, Waltham, MA, US) to label lysosomes and 0.02 ng/mL Hoechst 33342 for three hours to label the cell nucleus. After that, the media was removed, and cells were washed three times by PBS and fixed with paraformaldehyde 4% for 20 minutes. The cells were analyzed with an inverted fluorescence microscope (Nikon, Tokyo, Japan).

Abbreviations

MAGL: Monoacylglycerol lipase; CTAB: Cetyltrimethylammonium bromide; 2-AG: 2-arachidonoylglycerol; MPS: phagocyte system; HAS: albumin from human serum albumin; MAGL23-C: MAGL solubilized with CTAB; MAGL23-AC: MAGL solubilized with CTAB formulated with albumin; MAGL23-F: MAGL solubilized with Pluronic acid; MAGL23-AF; MAGL solubilized with pluonic acid formulated with albumin; XRD: X-ray diffractometer; FTIR: Fourier-transform infrared; TEM: transmission electron microscope; DLS: Dynamic light scattering; PBS: Phosphate-buffered saline; EPR: Enhanced Permeability Retention;

Declarations

Authors' contributions

All the authors contributed to design conduct experiments, analyzing data, and writing in manuscript.

Funding and Acknowledgements

This work was financially supported by SPIN-Supporting Principal Investigators, Ca'Foscari University of Venice, Italy; by MIUR (PRIN 2017, project 2017SA5837) and by the Italian Ministry of Health – Ricerca Finalizzata 2016 - NET-2016-02363765.

Consent for publication

All the authors read and approved the original draft of the manuscript and declare no competing/conflict of interests.

Availability of data and materials

The original data used in this manuscript are available from the corresponding author upon reasonable request.

Ethics approval and consent to participate

Not applicable

References

1. Verma S, Gokhale R, Burgess DJ. A comparative study of top-down and bottom-up approaches for the preparation of micro/nanosuspensions. Int. J. Pharm. 2009;380:216–22.
2. Kalepu S, Nekkanti V. Insoluble drug delivery strategies: Review of recent advances and business prospects. Acta Pharm. Sin. B. 2015;5:442–53.
3. Gupta S, Kesarla R, Omri A. Formulation Strategies to Improve the Bioavailability of Poorly Absorbed Drugs with Special Emphasis on Self-Emulsifying Systems. Corp. ISRN Pharm. Hindawi Publishing; 2013;2013:16.
4. Barbosa EJ, Löbenberg R, de Araujo GLB, Bou-Chacra NA. Niclosamide repositioning for treating cancer: Challenges and nano-based drug delivery opportunities. Eur. J. Pharm. Biopharm. 2019;141:58–69.
5. Hanahan D, Weinberg RA. Hallmarks of cancer: the next generation. Cell. 2011;144:646–74.
6. Falzone L, Salomone S, Libra M. Evolution of cancer pharmacological treatments at the turn of the third millennium. Front. Pharmacol. 2018. p. 1300.
7. Mirza AZ, Siddiqui FA. Nanomedicine and drug delivery: a mini review. Int. Nano Lett. Springer Nature; 2014;4:1–7.
8. Adeel M, Duzagac F, Canzonieri V, Rizzolio F. Self-Therapeutic Nanomaterials for Cancer Therapy: A Review. ACS Appl. Nano Mater. American Chemical Society; 2020;3:4962–71.
9. Fabbro D, Ruetz S, Buchdunger E, Cowan-Jacob SW, Fendrich G, Liebetanz J, et al. Protein kinases as targets for anticancer agents: From inhibitors to useful drugs. Pharmacol. Ther. Pergamon; 2002. p. 79–98.
10. Fleck R, Bach D. Trends in Personalized Therapies in Oncology: The (Venture) Capitalist's Perspective. J. Pers. Med. 2012;2:15–34.
11. Long JZ, Nomura DK, Cravatt BF. Characterization of Monoacylglycerol Lipase Inhibition Reveals Differences in Central and Peripheral Endocannabinoid Metabolism. Chem. Biol. NIH Public Access; 2009;16:744–53.
12. Nomura DK, Long JZ, Niessen S, Hoover HS, Ng SW, Cravatt BF. Monoacylglycerol Lipase Regulates a Fatty Acid Network that Promotes Cancer Pathogenesis. Cell. Cell; 2010;140:49–61.

13. Bononi G, Poli G, Rizzolio F, Tuccinardi T, Macchia M, Minutolo F, et al. An updated patent review of monoacylglycerol lipase (MAGL) inhibitors (2018-present). Expert Opin. Ther. Pat. Taylor and Francis Ltd.; 2020;31:153–68.
14. Granchi C, Rizzolio F, Palazzolo S, Carmignani S, MacChia M, Saccomanni G, et al. Structural Optimization of 4-Chlorobenzoylpiperidine Derivatives for the Development of Potent, Reversible, and Selective Monoacylglycerol Lipase (MAGL) Inhibitors. J. Med. Chem. 2016;59:10299–314.
15. Granchi C, Caligiuri I, Bertelli E, Poli G, Rizzolio F, Macchia M, et al. Development of terphenyl-2-methyloxazol-5(4 H)-one derivatives as selective reversible MAGL inhibitors. J. Enzyme Inhib. Med. Chem. 2017;32:1240–52.
16. Granchi C, Lapillo M, Glasmacher S, Bononi G, Licari C, Poli G, et al. Optimization of a Benzoylpiperidine Class Identifies a Highly Potent and Selective Reversible Monoacylglycerol Lipase (MAGL) Inhibitor. J. Med. Chem. 2019;62:1932–58.
17. Schlosburg JE, Blankman JL, Long JZ, Nomura DK, Pan B, Kinsey SG, et al. Chronic monoacylglycerol lipase blockade causes functional antagonism of the endocannabinoid system. Nat. Neurosci. 2010;13:1113–9.
18. Lepeltier E, Rijo P, Rizzolio F, Popovtzer R, Petrikaite V, Assaraf YG, et al. Nanomedicine to target multidrug resistant tumors. Drug Resist. Updat. Churchill Livingstone; 2020;52.
19. Rizzolio F. Nanomedicine in Cancer Pathology. Curr. Med. Chem. Bentham Science Publishers Ltd.; 2018;25:4190–1.
20. Bayda S, Hadla M, Palazzolo S, Riello P, Corona G, Toffoli G, et al. Inorganic Nanoparticles for Cancer Therapy: A Transition from Lab to Clinic. Curr. Med. Chem. 2017;25:4269–303.
21. Palazzolo S, Bayda S, Hadla M, Caligiuri I, Corona G, Toffoli G, et al. The Clinical Translation of Organic Nanomaterials for Cancer Therapy: A Focus on Polymeric Nanoparticles, Micelles, Liposomes and Exosomes. Curr. Med. Chem. 2017;25:4224–68.
22. Kumar V, Palazzolo S, Bayda S, Corona G, Toffoli G, Rizzolio F. DNA nanotechnology for cancer therapy. Theranostics. 2016. p. 710–25.
23. Müller RH, Gohla S, Keck CM. State of the art of nanocrystals - Special features, production, nanotoxicology aspects and intracellular delivery. Eur. J. Pharm. Biopharm. 2011. p. 1–9.
24. Liu F, Park JY, Zhang Y, Conwell C, Liu Y, Bathula SR, et al. Targeted cancer therapy with novel high drug-loading nanocrystals. J. Pharm. Sci. John Wiley and Sons Inc.; 2010;99:3542–51.
25. Fontana F, Figueiredo P, Zhang P, Hirvonen JT, Liu D, Santos HA. Production of pure drug nanocrystals and nano co-crystals by confinement methods. Adv. Drug Deliv. Rev. 2018;131:3–21.
26. Du J, Li X, Zhao H, Zhou Y, Wang L, Tian S, et al. Nanosuspensions of poorly water-soluble drugs prepared by bottom-up technologies. Int. J. Pharm. Elsevier; 2015. p. 738–49.
27. Park J, Sun B, Yeo Y. Albumin-coated nanocrystals for carrier-free delivery of paclitaxel. J. Control. Release. Elsevier B.V.; 2017;263:90–101.

28. Mahesh KV, Singh SK, Gulati M. A comparative study of top-down and bottom-up approaches for the preparation of nanosuspensions of glipizide. Powder Technol. Elsevier; 2014;256:436–49.
29. Walkey CD, Olsen JB, Guo H, Emili A, Chan WCW. Nanoparticle size and surface chemistry determine serum protein adsorption and macrophage uptake. J. Am. Chem. Soc. 2012;134:2139–47.
30. Hatakeyama H, Akita H, Harashima H. The polyethyleneglycol dilemma: Advantage and disadvantage of PEGylation of liposomes for systemic genes and nucleic acids delivery to tumors. Biol. Pharm. Bull. 2013. p. 892–9.
31. Stehle G, Sinn H, Wunder A, Schrenk HH, Stewart JCM, Hartung G, et al. Plasma protein (albumin) catabolism by the tumor itself - Implications for tumor metabolism and the genesis of cachexia. Crit. Rev. Oncol. Hematol. Elsevier; 1997. p. 77–100.
32. Parodi A, Miao J, Soond SM, Rudzińska M, Zamyatnin AA. Albumin nanovectors in cancer therapy and imaging. Biomolecules. MDPI AG; 2019;9.
33. Hoogenboezem EN, Duvall CL. Harnessing albumin as a carrier for cancer therapies. Adv. Drug Deliv. Rev. Elsevier B.V.; 2018. p. 73–89.
34. Li C, Wang X, Song H, Deng S, Li W, Li J, et al. Current multifunctional albumin-based nanoplatforms for cancer multi-mode therapy. Asian J. Pharm. Sci. Shenyang Pharmaceutical University; 2020. p. 1–12.
35. Manallack DT, Prankerd RJ, Yuriev E, Oprea TI, David K. The Significance of Acid/Base Properties in Drug Discovery. Chem Soc Rev. 2014;42:485–96.
36. Baba K, Pudavar HE, Roy I, Ohulchanskyy TY, Chen Y, Pandey RK, et al. New method for delivering a hydrophobic drug for photodynamic therapy using pure nanocrystal form of the drug. Mol. Pharm. 2007;4:289–97.
37. Rodig OR. Spectrometric Identification of Organic Compounds. J. Med. Chem. 8th ed. 1963;6:826–7.
38. National Institute of Standards and Technology. NIST Chemistry WebBook, SRD 69. U.S Dep. Commer. 2018;1.
39. MADEJOVA J, KOMADEL P. Baseline studies of the clay minerals society source clays: Introduction. Clays Clay Miner. 2001;49:410–432.
40. Dizaj SM, Vazifehasl Z, Salatin S, Adibkia K, Javadzadeh Y. Nanosizing of drugs: Effect on dissolution rate. Res. Pharm. Sci. 10:95–108.
41. Wolinsky JB, Colson YL, Grinstaff MW. Local drug delivery strategies for cancer treatment: Gels, nanoparticles, polymeric films, rods, and wafers. J. Control. Release. 2012;159:14–26.
42. Kratz F. A clinical update of using albumin as a drug vehicle - A commentary. J. Control. Release. Elsevier; 2014. p. 331–6.
43. Gil-Ordóñez A, Martín-Fontecha M, Ortega-Gutiérrez S, López-Rodríguez ML. Monoacylglycerol lipase (MAGL) as a promising therapeutic target. Biochem. Pharmacol. Elsevier Inc.; 2018. p. 18–32.
44. Poli G, Lapillo M, Jha V, Mouawad N, Caligiuri I, Macchia M, et al. Computationally driven discovery of phenyl(piperazin-1-yl)methanone derivatives as reversible monoacylglycerol lipase (MAGL)

inhibitors. J. Enzyme Inhib. Med. Chem. Taylor and Francis Ltd; 2019;34:589–96.

45. Ji Z, Shen Y, Feng X, Kong Y, Shao Y, Meng J, et al. Deregulation of Lipid Metabolism: The Critical Factors in Ovarian Cancer. Front. Oncol. 2020.
46. Pagano E, Borrelli F, Orlando P, Romano B, Monti M, Morbidelli L, et al. Pharmacological inhibition of MAGL attenuates experimental colon carcinogenesis. Pharmacol. Res. 2017;119:227–36.
47. Elluru M, Ma H, Hadjiargyrou M, Hsiao BS, Chu B. Synthesis and characterization of biocompatible hydrogel using Pluronics-based block copolymers. Polymer (Guildf). Elsevier Ltd; 2013;54:2088–95.
48. Oyama J, Lera-Nonose DSSL, Ramos-Milaré ÁCFH, Padilha Ferreira FB, de Freitas CF, Caetano W, et al. Potential of Pluronics ® P-123 and F-127 as nanocarriers of anti-Leishmania chemotherapy. Acta Trop. Elsevier; 2019;192:11–21.
49. Elsadek B, Kratz F. Impact of albumin on drug delivery - New applications on the horizon. J. Control. Release. 2012;157:4–28.
50. Peng Q, Zhang S, Yang Q, Zhang T, Wei XQ, Jiang L, et al. Preformed albumin corona, a protective coating for nanoparticles based drug delivery system. Biomaterials. 2013;34:8521–30.
51. Komarova Y, Malik AB. Regulation of endothelial permeability via paracellular and transcellular transport pathways. Annu. Rev. Physiol. 2009. p. 463–93.
52. Minshall RD, Malik AB. Transport across the endothelium: Regulation of endothelial permeability. Handb. Exp. Pharmacol. 2006;

Figures

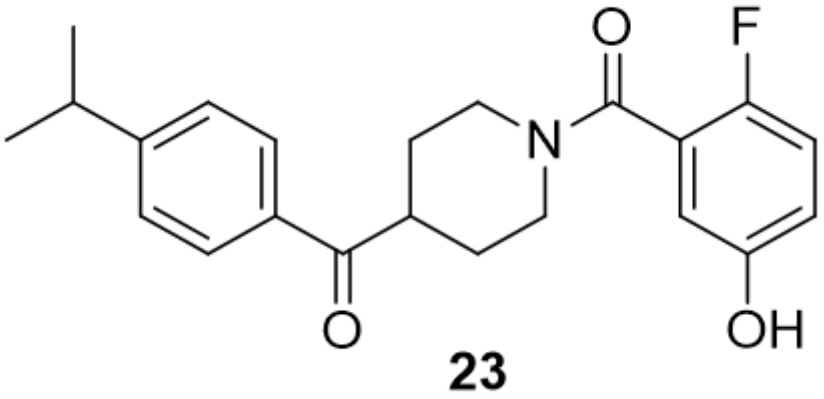

Figure 1

Chemical structure of MAGL23.

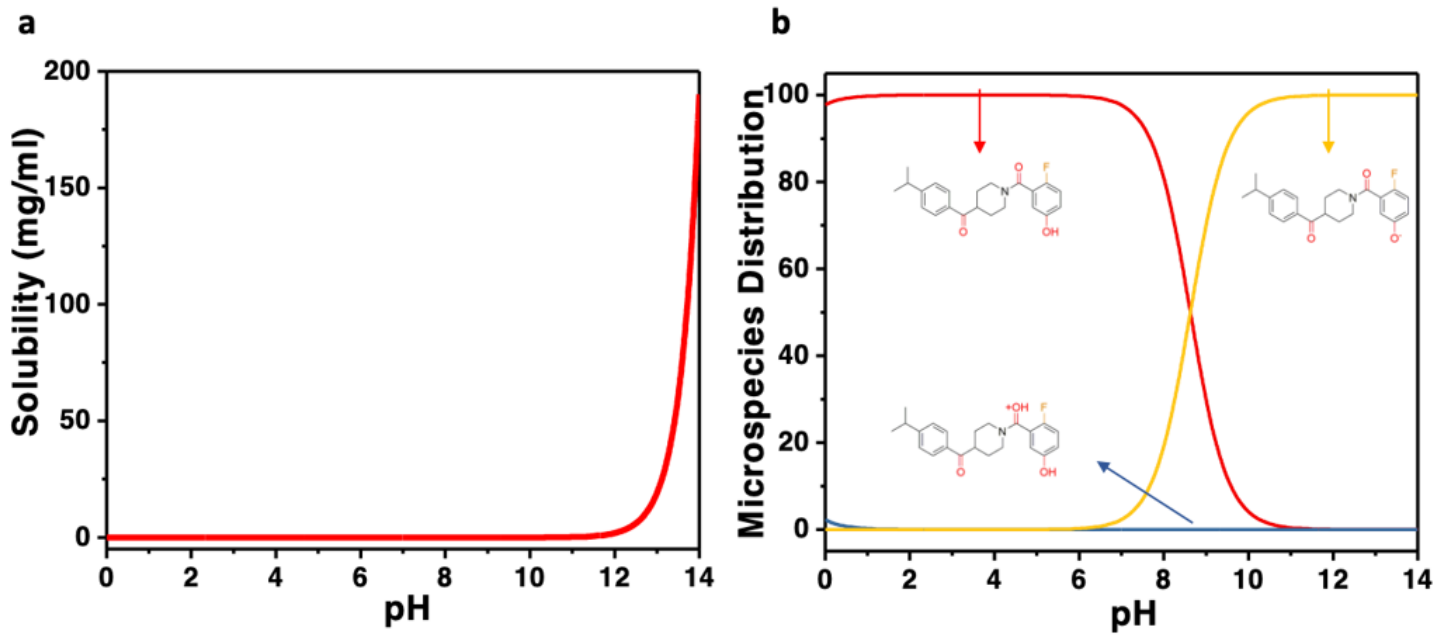

Figure 2

a) Solubility vs pH trends (predicted by Chemicalize.com). b) Microspecies distribution at different pH values, where microspecies in red is the neutral one, in blue is protonated at the oxygen of the amide carbonyl group (basic moiety) and in yellow is deprotonated in the phenolic group (acid moiety) (predicted by Chemicalize.com).

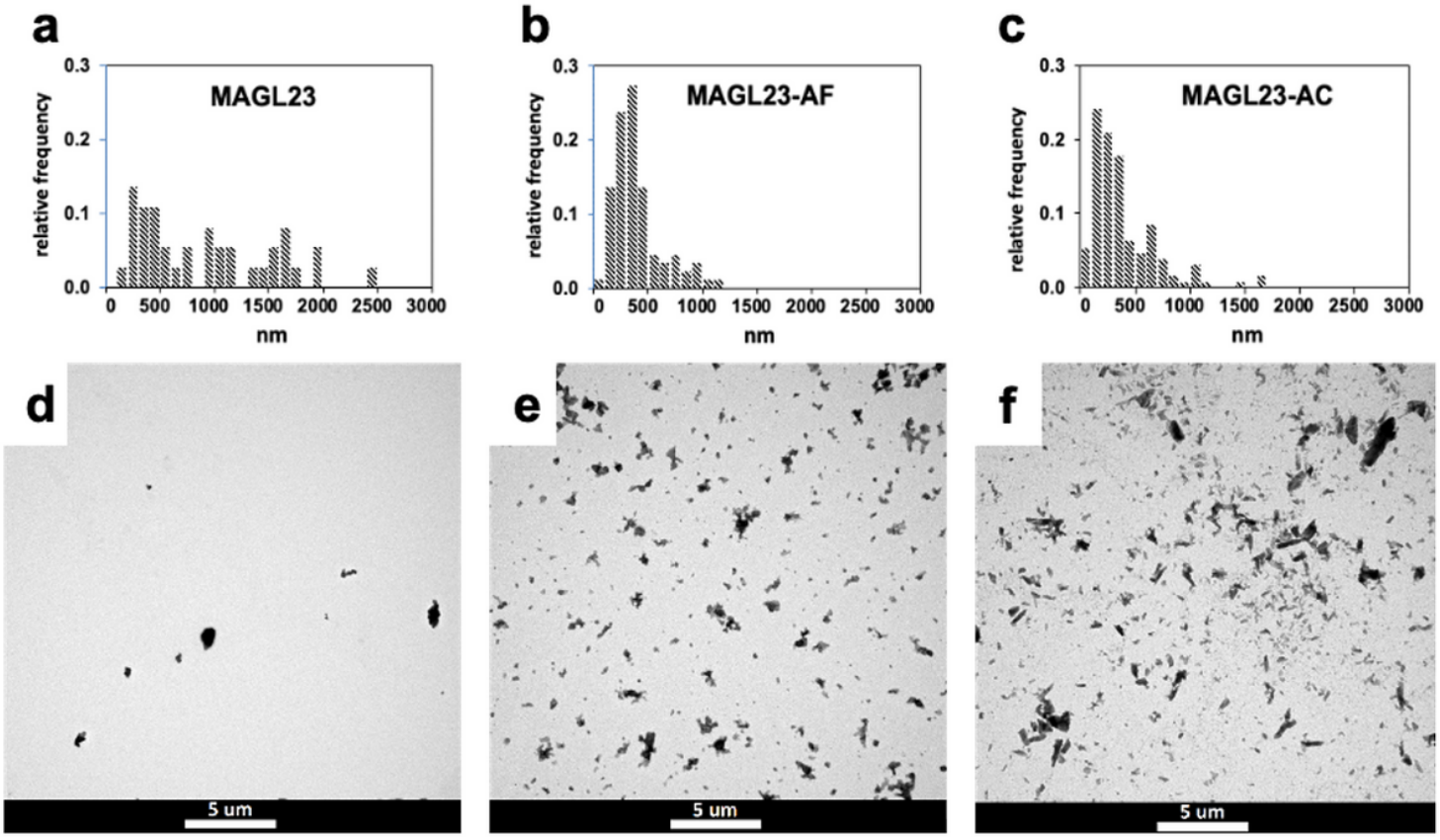

Figure 3

(a,b,c) Relative frequency of crystals size of MAGL23, MAGL23-AF and MAGL23-AC from left to right; (d,e,f) TEM images of MAGL23, MAGL23-AF and MAGL23-AC.

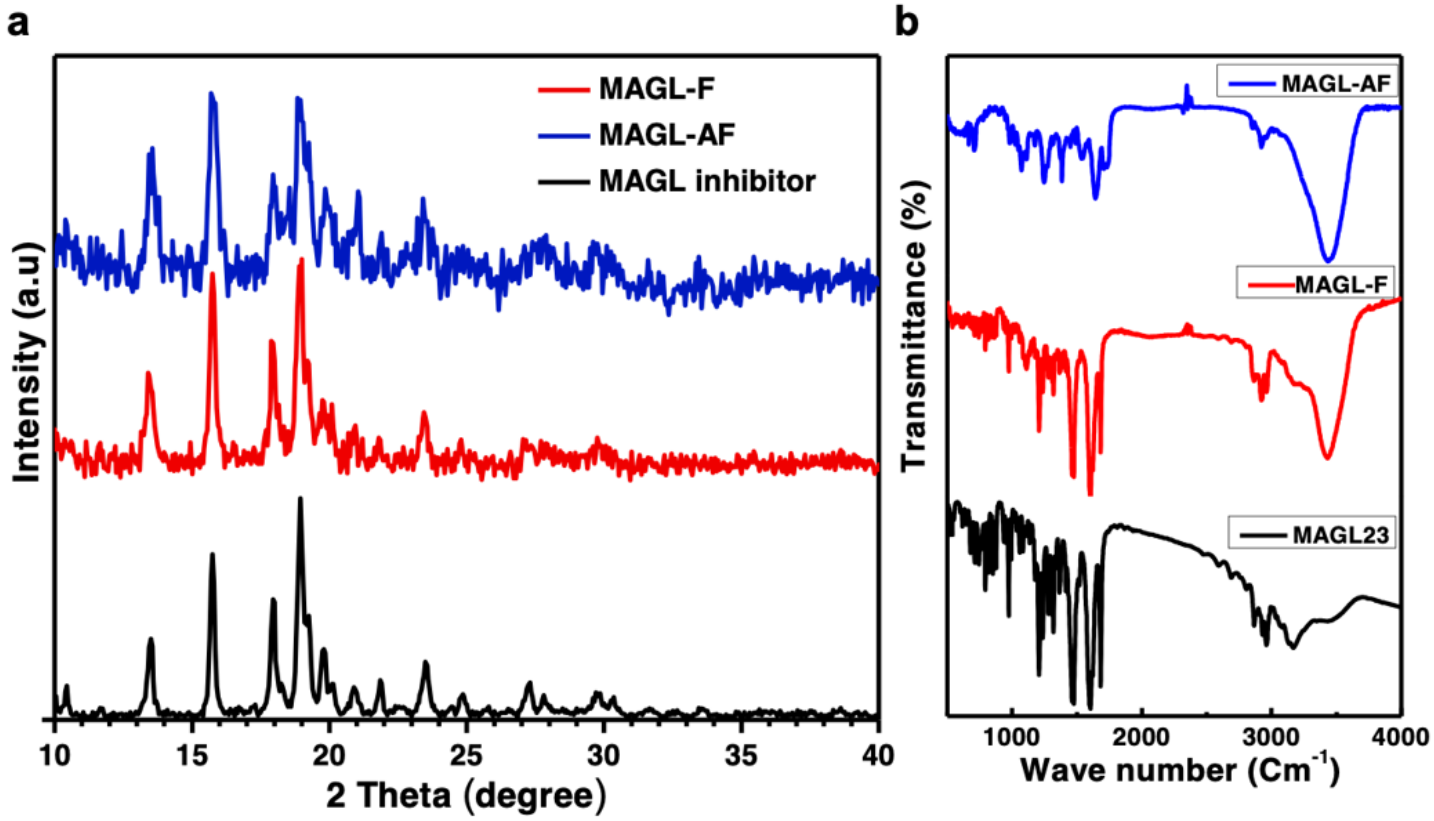

Figure 4

a) XRD diffractograms and b) FTIR spectra of MAGL23 (drug powder) and nanocrystals at different formulation steps.

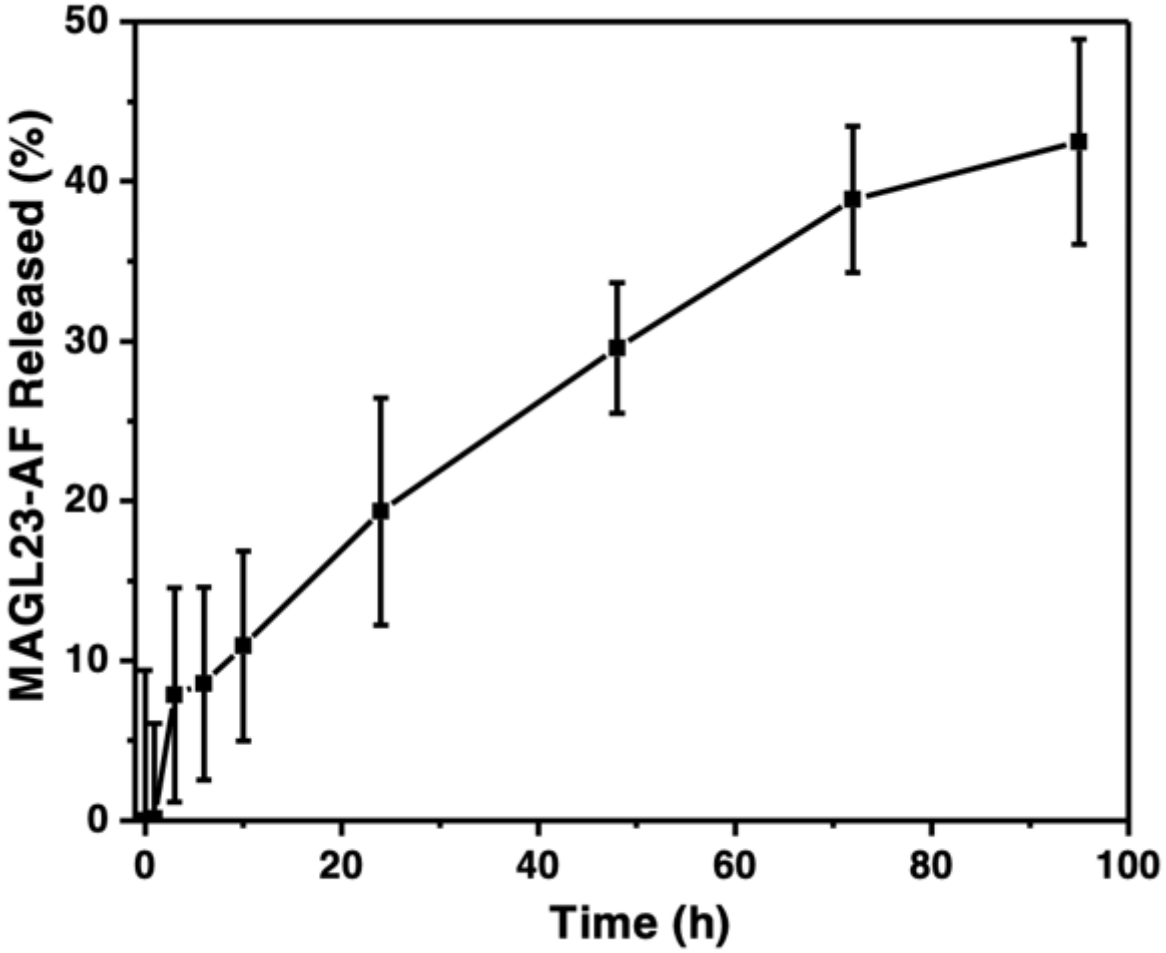

Figure 5

Release profile of MAGL23-AF reported as percentage of drug released percentage (%) over time (h).

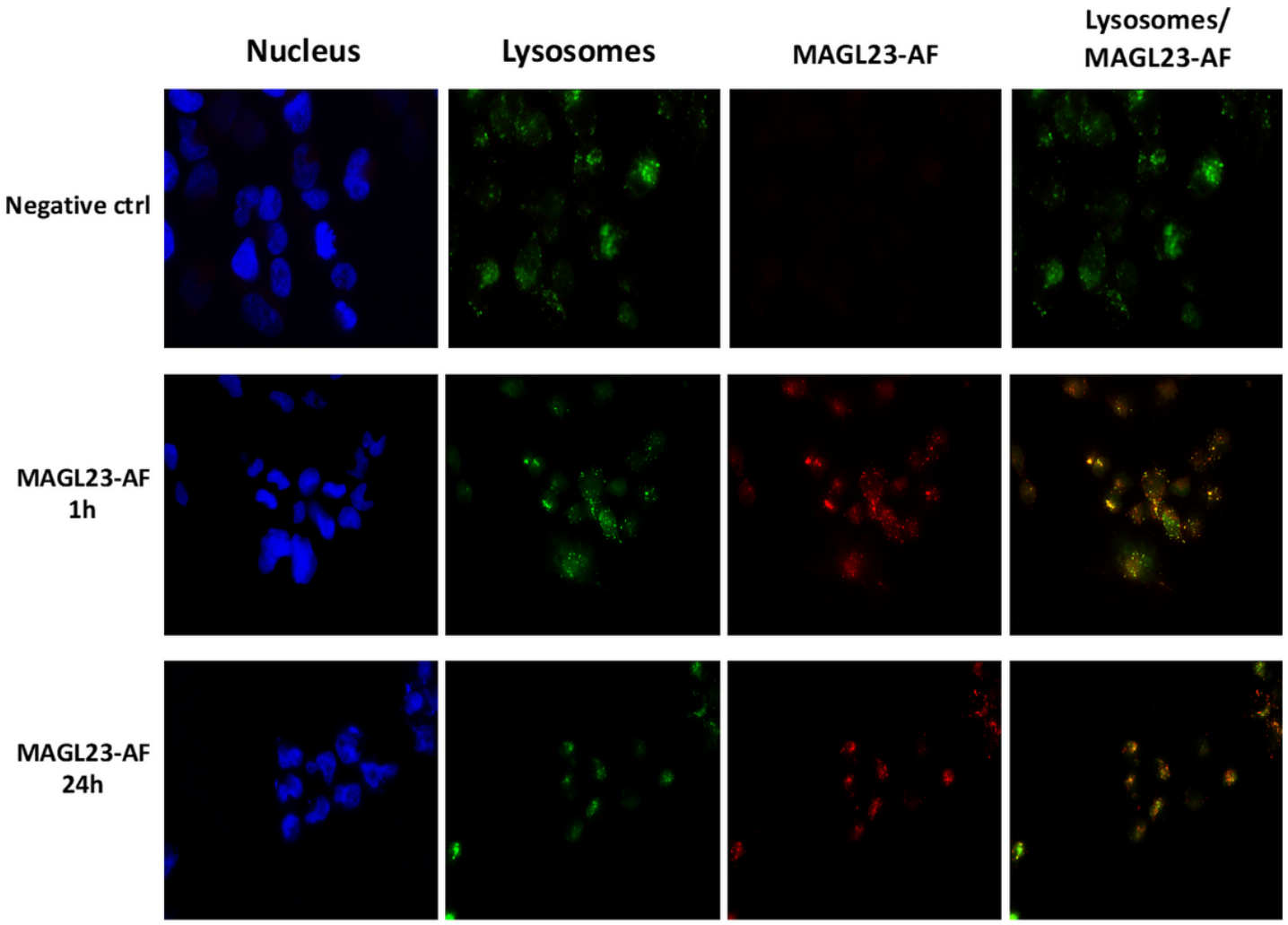

Figure 6

Cell internalization study of MAGL23-AF nanocrystals at different time points. Nucleus (blue) were stained with Hoechst 33342; Lysosomes (green) were stained with Lysotracker; MAGL23-AF were stained with Rhodamine. Yellow color implied colocalization between lysosomes and MAGL23-AF.

Supplementary Files

This is a list of supplementary files associated with this preprint. Click to download.

- GraphicalAbstract.png
- supportinginfo1.docx